A simple contaminant fate and transport modelling tool for management and risk assessment of groundwater pollution from contaminated sites

Luca Locatelli[a,b], Philip J. Binning[a], Xavier Sanchez-Vila[b], Gitte Lemming Søndergaard[a], Louise Rosenberg[a], Poul L. Bjerg[a]

[a] Technical University of Denmark, Dept. of Environmental Engineering, Bygningstorvet, Building 115, 2800 Kgs Lyngby, Denmark
[b] Universitat Politècnica de Catalunya, Dept of Civil and Environmental Engineering, C. Jordi Girona 1-3, 08034 Barcelona, Spain

Corresponding author: Luca Locatelli
E-mail: lulo@env.dtu.dk

Abstract

Contaminated sites pose a significant threat to groundwater resources. The resources that can be allocated by water regulators for site investigation and cleanup are limited compared to the large number of contaminated sites. Numerical transport models of individual sites require large amounts of data and are labor intensive to set up, and thus they are likely to be too expensive to be useful in the management of thousands of contaminated sites. Therefore, simple tools based on analytical solutions of contaminant transport models are widely used to assess (at an early stage) whether a site might pose a threat to groundwater. We present a tool consisting of five different models, representing common geological settings, contaminant pathways, and transport processes. The tool employs a simplified approach for preliminary, conservative, fast and inexpensive estimation of the contamination levels of aquifers. This is useful for risk assessment applications or to select and prioritize the sites, which should be targeted for further investigation. The tool is based on steady-state semi-analytical models simulating different contaminant transport scenarios from the source to downstream groundwater, and includes both unsaturated and saturated transport processes. The models combine existing analytical solutions from the literature for vertical (from the source to the top of the aquifer) and horizontal (within the aquifer) transport. The effect of net recharge causing a downward migration and an increase of vertical dispersion and dilution of the plume is also considered. Finally, we illustrate the application of the tool for a preliminary assessment of two contaminated sites in Denmark and compare the model results with field data. The comparison shows that a first preliminary assessment with conservative, and often non-site specific parameter selection, is qualitatively consistent with broad trends in observations and provides a conservative estimate of contamination.

Keywords: Contaminant fate and transport; Risk assessment; Contaminant mass discharge; Analytical models; Groundwater pollution

1. Introduction

Approximately 2.5 million potential contaminated sites are estimated to be present in the EU, and 342,000 of those have already been identified (European Environment Agency, 2015). In Denmark, more than 35,000 contaminated sites are now registered, and this number has been steadily increasing over the last decade (Danske Regioner, 2017). Contaminated sites pose a threat to groundwater bodies, surface water ecosystems, drinking water supplies, soils, and human health. Remediation and investigation costs are generally high, and efforts must be made to prioritize sites and allocate funding for remediation according to the evaluation of potential hazards and the assessment of associated risks. Yet, risk assessment efforts are expensive, time and resource consuming, when considering the large number of sites at the regional or national scales. Therefore, simple and inexpensive tools for assessing the potential risk of contaminated sites to water bodies are essential (Bardos et al, 2016; Harclerode et al., 2016).

Overall, there is a need to provide fast evaluations that go beyond subjective risk assessment. For this purpose, it is very valuable to have simple analytical models that can be used for preliminary estimation of the contamination levels in aquifers threatened by contaminated sites. Most of the simple models in the literature employ the Advection Dispersion Equation incorporating a term for first order degradation (ADE1). These can be found in classic hydrogeology textbooks and early compilation works, such as those of Hunt (1978), assuming horizontal flow (in 3D) and steady state transport conditions. Wexler (1992) later compiled the analytical solutions available at that time, and presented additional analytical solutions (in 1D, 2D and 3D) of the ADE1 for finite, semi-finite, or infinite aquifers, constant or time-dependent sources (either uniform or spatially distributed), and accounting for a number of boundary conditions.

In recent years, more involved solutions have been presented dealing with horizontal flow: Srinivasan and Clement (2008a; 2008b) provided solutions for sequential coupled one-dimensional transport considering time-dependent input point sources; Simpson and Ellery (2014) extended this work to provide the solution in terms of series expansions. Sun et al. (1999a; 1999b) provided steady-state solutions in 3D for complex reactive systems with sequential reactions taking place either in series or in parallel for constant input. Extensions of this work to 1D, 2D and 3D transient transport, with constant or pulse input point sources were provided by Bauer et al. (2001) and Sudicky et al. (2013). Paladino et al. (2018) provide solutions for 3D transport from plane sources with both contaminant concentrations and mass discharge inputs with an exponential decay.

For vertical flow, Chambon et al. (2011) and Troldborg et al. (2009) presented analytical solutions of the ADE1 for simulating contaminant transport in fractured clay tills and unsaturated zones, respectively. The former work is 1D and includes solutions for both constant and pulse plane sources, while the latter provides 3D solutions.

Analytical solutions of solute transport are useful for risk evaluations and management of water resources. They provide easy-to-use and fast evaluations, allowing efficient estimation of risk under different conditions (Zarlenga et al., 2016; Troldborg et al., 2009). Existing risk assessment tools generally employ simplified homogeneous models and analytical or semi-analytical solutions. Table 1 includes a description of the main features of a variety of existing risk assessment tools. RISC5 was developed for conventional forward and backward risk calculations and it is based on analytical solutions of the ADE1 based on superposition. BIOCHLOR and REMChlor are tools developed by the US Environmental Protection Agency and designed for assessing the fate and transport of chlorinated solvents in aquifers for a constant source, and steady-state transport. ConSim, BioBalance, CoronaScreen and ROME are also based on analytical solutions to compute concentrations in aquifers including vertical and horizontal transport, either in 2D or 3D. PLUME (Wagner, 1985) simulates transport in aquifers based on 3D analytical solutions of the horizontal flow ADE1. The assessment of risk for real sites can require calculations accounting for the actual geological heterogeneity, and uncertainty in inputs and parameters. In these cases, the calculations can be done at different levels, with a first assessment employing simple analytical approaches (de Barros et al., 2011).

Table 1. Examples of existing risk assessment models incorporating analytical solutions to simulate contaminant concentrations in soils and groundwater downstream a contaminant source.

	Input source type: Steady-state (S); transient (T)	Transport: Vertical (V); Horizontal (H)	Dimensionality of the horizontal transport model	Degradation
RISC5 (Risk 5, 2011)	S; T	V; H	3D	first order
BIOCHLOR (Aziz et al., 2000)	S	H	3D	first order, sequential
REMChlor (Falta et al., 2007)	S; T	H	3D	first order, sequential
ConSim (Davison and Hall, 2003)	S; T	V; H	2D	first order
BioBalance (Kamath et al., 2006)	S; T	V; H	3D	first order
CoronaScreen (Thornton et al, 2017; Wilson et al, 2017)	S; T	H	3D	first order
ROME (ANPA, 2002)	S	V; H	3D	first order
PLUME (Wagner, 1985)	S; T	H	3D	first order

Leaching into the underlying aquifer is governed by the actual geological setting, pathways, contaminant properties and fate and transport processes. It is crucial that the applied transport models for risk assessment cover a broad range of conceptual models in a systematic way. None of the tools/solutions presented in Table 1 can be applied to significantly different geological conditions and are often restricted in the types of contaminants that can be considered. In particular, they do not combine different vertical and horizontal transport models and the processes of advection, dispersion, air diffusion, degradation and sequential degradation. These combinations are generally relevant to simulate concentrations in aquifers downstream of contaminant sources.

In this work, we focus on the preliminary assessment of potential aquifer pollution from contaminated sites. A common approach to aquifer risk assessment considers a groundwater body to be contaminated if the simulated pollutant concentrations at a predefined control Point of Compliance (POC), located downstream the site, exceeds a quality criteria (typically a given threshold for human health). The risk can be assessed for concentration thresholds, as is common practice in many countries (Bardos et al., 2002; Miljøstyrelsen, 2016). This is different from approaches where the risk assessment includes a calculation in terms of probability (e.g., cancer, see Andricevic and Cvetkovic 1996; Lemming et al., 2010).

Contaminant mass discharge has also been accepted as an alternative to point-value concentration-based risk assessment (Cremeans et al., 2018; Schwede and Cirpka, 2010; Basu et al., 2006), because mass discharge provides an integrated assessment of the impact of contamination on water resources. Contaminant mass discharge is also useful for comparing risks from different sites, or prioritization of risk at the catchment scale (Troldborg et al., 2008).

In this paper we present a new tool for risk assessment applications and management of groundwater pollution from contaminated sites. The new tool starts with a process of conceptualization, defining a number of models that can be considered representative of the majority of contaminated sites, including common types of geologies, and contaminant transport and fate processes. The models proposed combine different conceptualizations of source characteristics. All the models employ plane sources with both contaminant concentration and mass discharge inputs. Vertical downward transport through the unsaturated/saturated zone (from a source located at the surface to the top of the underlying aquifer) is coupled to horizontal (3D) transport in the aquifer under the influence of natural recharge (causing a downward migration, enhancing plume dispersion). The models presented in this study are intended to be used in a regulatory context and aim at providing a first conservative and early stage assessment based on generally sparse data. Therefore, closed-form analytical (or semi-analytical) steady-state solutions are preferred. These are simple to use, easy to implement, computationally fast, and require both minimal amounts of data and limited software knowledge.

An important consideration is uncertainty, as shown in the literature on stochastic modeling (e.g., Ciriello et al., 2017; Zarlenga et al., 2017; Fernandez-Garcia et al., 2012). This literature shows that uncertainty is important when evaluating the probability of system failure for a given site, improving risk assessment, with significant economic and social implications. Here, however, we do not use stochastic models. Instead, we use conservative assumptions and simplifications of a real system when treating uncertainty and when selecting model structure. In this way, the tool can provide a conservative point-value concentration at the POC or contaminant mass discharge at a control plane. This preliminary assessment would typically need to be extended to more detailed analyses for sites that are considered more critical, and would require more resources. However, such an extended analysis is beyond the scope of this paper.

Finally, the tool presented here is applied to two contaminated sites in Denmark in order to show the model applicability. Here, we demonstrate in a simple way how uncertainty in the conceptualization (source location) can be addressed. Results from the simulations are compared with groundwater concentration data. The objective of the comparison is only to illustrate and discuss whether a first and conservative parameter selection would actually produce a conservative estimation of aquifer pollution useful for first screening/assessment purposes.

2. Methods

2.1 The contaminant fate and transport modelling tool

Being a tool for risk assessment applications, screening purposes and preliminary and fast evaluations, the idea is to simplify the huge wide picture of geological types, source distribution, flow direction, etc. into a minimum number of models. These models should be able to simulate the most relevant processes combining different conceptualizations of source characteristics, vertical downward transport through the unsaturated/saturated zone towards the top of the aquifer, and horizontal transport in the aquifer. Five models were found to be sufficient to simulate most situations.

The five models selected were developed by combining (and slightly modifying) published analytical solutions, and particularly, by coupling solutions of vertical transport (from a source to the top of the underlying aquifer) and horizontal transport (within an aquifer). The 3D horizontal transport solutions are modified to account for the effect of groundwater recharge that causes a downward migration and an increase of vertical dispersion and dilution of the plume as it is transported downstream in the aquifer.

2.2 Conceptualization

All the models considered have a number of common features: they incorporate analytical and semi-analytical steady-state solutions to compute aqueous phase concentrations from a planar source to a downstream point of compliance in an aquifer. The five selected models include the most common contaminant transport mechanisms and processes at contaminated sites: advection, dispersion, degradation, sequential degradation and air diffusion. Sorption processes are not included as they do not affect steady-state solutions of the advection-dispersion equation when degradation is assumed to occur only in the aqueous phase.

The following assumptions apply:

- Homogenous conditions. All soil/aquifer parameters (e.g. water content, porosity, dispersivity, etc.) and contaminant properties/parameters (e.g. diffusion coefficients, dimensionless Henry's law constants, degradation rates, etc.) are constant in space and time.
- Advection only occurs in the aqueous phase with a constant velocity and has either a vertical or a horizontal flow direction.
- Degradation is described by first order kinetics and only occurs in the aqueous phase.
- The concentration and the contaminant mass discharge describing the contaminant source are constant over time.
- The models simulate only contaminants in the aqueous and gas phases. However, they can also be used for a first assessment of non-aqueous phase liquid transport as shown in the result section.

These assumptions/limitations are reasonable since the models are meant for risk assessment applications which require simple conceptual models and must be designed to require little data. Further assumptions are specified for some of the models.

Steady-state solutions were chosen, because contaminant source concentration and mass discharge over time are not well known at most contaminated sites, making it hard to justify the need for time-dependent approaches. Furthermore, many contaminant sources are old and have been actively discharging contaminants for decades, meaning that the concentrations in aquifers up to few hundred meters downstream are likely to have reached quasi steady-state concentrations. Steady-state models can significantly overestimate concentrations of highly sorbing compounds like heavy metals that are not likely to reach steady-state concentrations at a point of compliance downstream in the aquifer because of the slow transport time compared to the release time from the source.

The tool can be used to provide first estimates of concentrations at a point of compliance using a conservative approach. If the concentration values simulated at the POC are lower than the target (predefined) values, then the site is likely to pose no risk. Otherwise, more detailed site assessment might be required, including for example, source characterization and the development of a full transient model, historical information with detailed geology, and accounting for uncertainty. For screening purposes, the parameters should be selected to provide the maximum potential values. This means that when a range of realistic values is available for a given parameter, the screening should use the value that provides the largest concentration values, e.g., the smallest dispersity, or the smallest degradation rate. However, this can be difficult because some parameters are inversely correlated. For example, high groundwater velocities enhance dilution and spreading, but result in small degradation due to short travel times.

2.3 The conceptual frame models

This section presents the five contaminant transport models (*Models I to V*). *Models I-IV* consist of coupled vertical and horizontal transport models, and *Model V* considers only horizontal transport in an aquifer. Figure 1 to Figure 5 show conceptual sketches of the 5 models. *Model I* describes transport from contaminant sources located in a homogeneous aquitard overlying an aquifer. *Model II* idealizes sources located in fractured saturated aquitards overlying an aquifer. *Model III* deals with contaminant sources with volatile compounds located in an unsaturated zone overlying an unconfined aquifer. *Model IV* represents sources with volatile compounds in an unsaturated zone located under an impervious area that inhibits infiltration, so that only vapor phase diffusion occurs in the unsaturated zone (no advection in water). *Model V* considers contaminant sources in direct contact with the groundwater. Table 2 provides a summary of the five models and their main characteristics.

The models include a user specified rectangular source area of length Lx and width Ly (except for *Model IV* that has a circular area of radius R_1) with a uniform distributed concentration C_0 (in *Model V* $C_0 = C_1$) and water infiltration rate I (except for *Model IV* where $I=0$). The source water infiltration rate I can be different from the recharge over the aquifer I_R. Thereby, a contaminant mass discharge input can be estimated at the source. At the POC both the contaminant concentration and the contaminant mass discharge (over a control plane) can be calculated, which can be used for assessing the actual risk at the site.

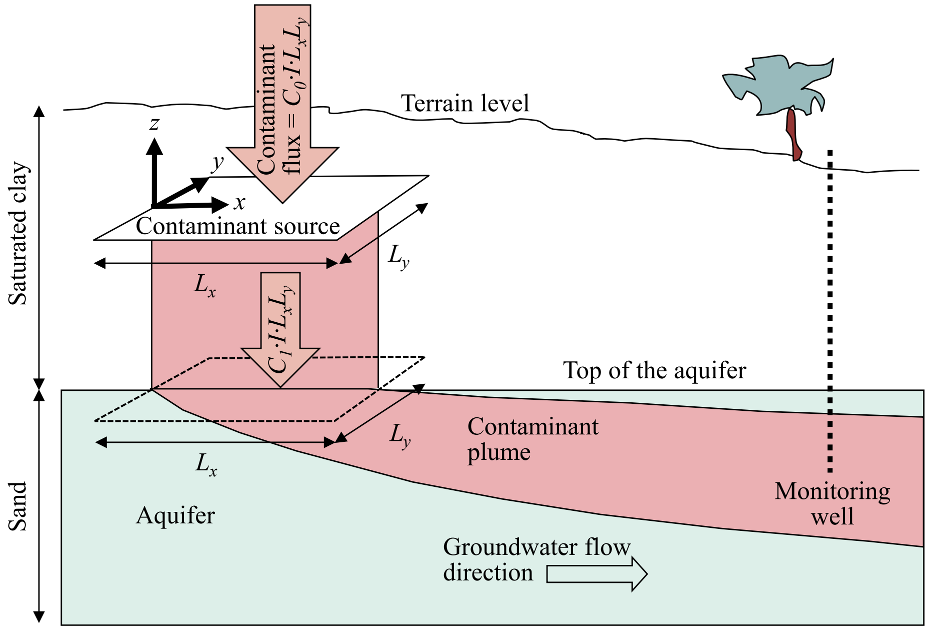

Figure 1. Model I. Vertical contaminant transport from a source located in a homogeneous saturated clay, downward to the top of the aquifer and then horizontal transport in the aquifer.

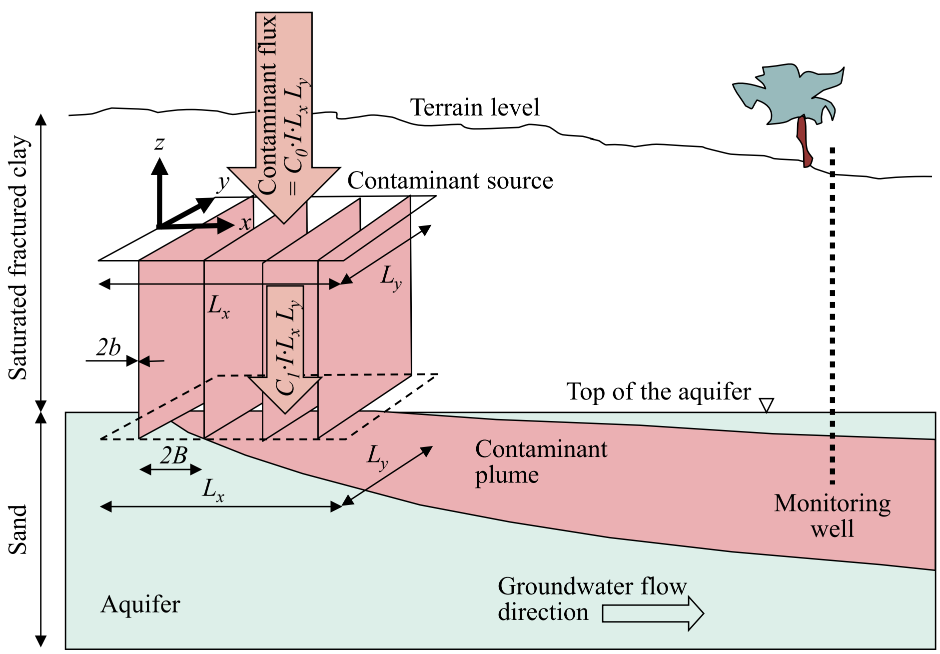

Figure 2. Model II. Contaminant transport from a source located in a fractured saturated clay, downward to the top of the aquifer and then horizontal transport in the aquifer.

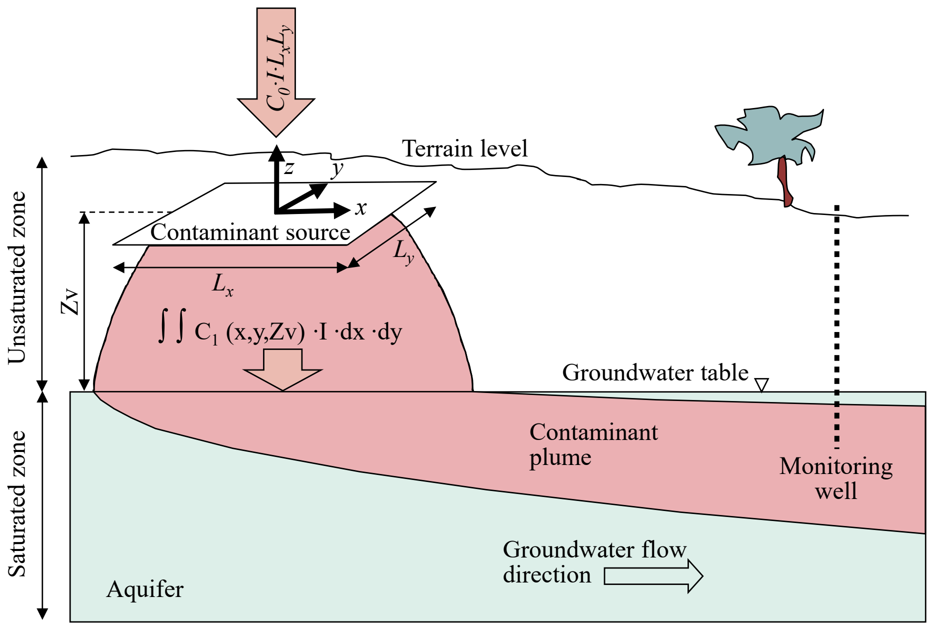

Figure 3. Model III. Contaminant transport from a source located in the unsaturated zone, downward to the top of the unconfined aquifer and then horizontal transport in the aquifer.

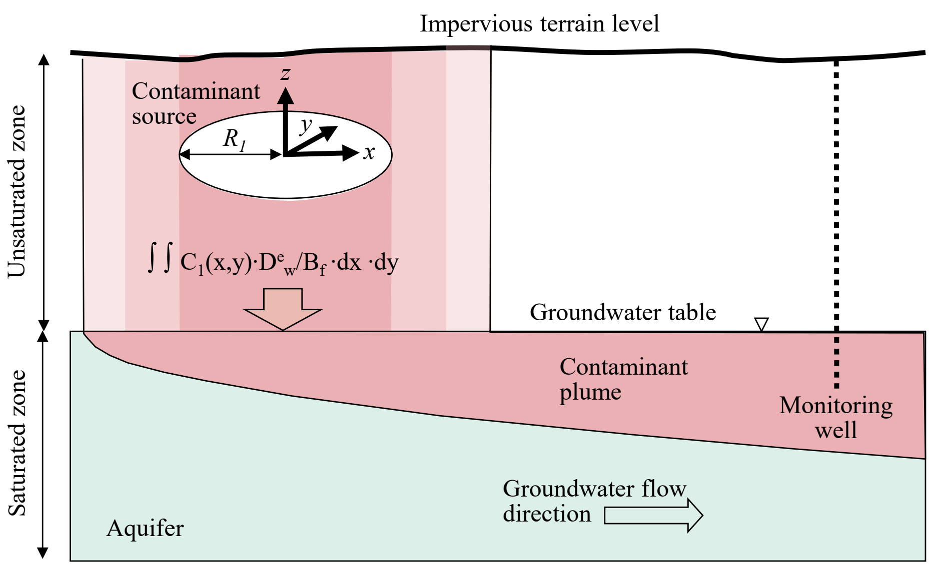

Figure 4. Model IV. Contaminant gas phase transport from a source located in an unsaturated zone below an impervious area (without downward water advection), to the top of the underlying aquifer and then horizontal transport in the aquifer.

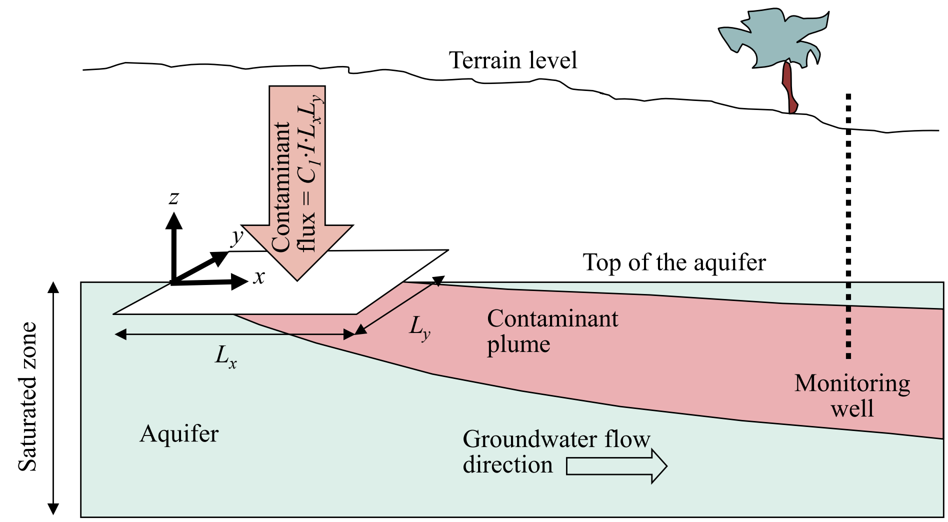

Figure 5. Model V. Horizontal contaminant transport from a source located at the top of the aquifer.

Table 2. Summary of the 5 steady-state contaminant transport models.

	Geology type	Vertical transport	Horizontal transport
Model I	Homogeneous saturated aquitard overlying an aquifer	1D aqueous phase transport including advection, dispersion, degradation and sequential degradation.	2D and 3D aqueous phase transport including advection, dispersion, degradation and sequential degradation. The contaminant mass discharge to the aquifer is uniform over a rectangular source area.
Model II	Fractured saturated clay overlying an aquifer	1D aqueous phase transport including advection, dispersion, degradation and sequential degradation.	2D and 3D aqueous phase transport including advection, dispersion, degradation and sequential degradation. The contaminant mass discharge to the aquifer is uniform over a rectangular source area.
Model III	Unsaturated zone overlying an unconfined aquifer	3D aqueous phase transport including advection, dispersion, air diffusion, and degradation (no sequential degradation).	2D and 3D aqueous phase transport including advection, dispersion, degradation and sequential degradation. The contaminant mass discharge to the aquifer is spatially distributed over the top of the aquifer.
Model IV	Unsaturated zone under an impervious area with zero infiltration overlying an unconfined aquifer	1D aqueous phase transport including dispersion, air diffusion, and degradation (no sequential degradation).	2D and 3D aqueous phase transport including advection, dispersion, degradation and sequential degradation. The contaminant mass discharge to the aquifer is spatially distributed over the top of the aquifer.
Model V	Direct input from the source to the groundwater aquifer	None	2D and 3D aqueous phase transport including advection, dispersion and sequential first order degradation. The contaminant mass discharge to the aquifer is uniform over a rectangular source area.

In the following, we present the model input parameters; the horizontal and vertical transport models and the coupling between them; and the sequential degradation model.

2.4 Model input parameters

Table 3 shows all the model parameters for *Model I* to *V*. The input parameters and variables in the table are divided into three categories: *Global parameters* applicable to both the vertical and the horizontal transport model, *Vertical model* parameters, and *Horizontal model* parameters.

Table 3. Model input parameters.

	Parameter	Description	Model				
			I	II	III	IV	V
Global parameters	Y_i [-]	Stoichiometric ratio of the i^th^ compound of the degradation chain = molar mass^{i+1}/molar mass^{i}. ($Y_1=1$)	x	x	x	x	x
	I [L/T]	Infiltration at the source	x	x	x		x
	L_x [L]	Source length	x	x	x		x
	L_y [L]	Source width	x	x	x		x
	R_1 [L]	Radius of the source				x	
	$C_{0\,i}$ [M/L^3]	Aqueous phase concentration at the source of the ith compound	x	x	x	x	x*
Vertical model	$k\_{v\,i}$ [T-1]	First order degradation rate of the ith compound	x	x	x	x	
	n_v [-]	Porosity	x	x	x	x	
	α_{L_v} [L]	Longitudinal dispersivity (z direction)	x		x		
	Z_v [L]	Distance between the source and the top of the aquifer	x	x	x		
	D_{w_v} [L^2/T]	Free diffusion coefficient in water	x	x			
	$2B\_v$ [L]	Fracture spacing		x			
	$2b\_v$ [L]	Fracture aperture		x			
	K_{b_v} [L/T]	Bulk hydraulic conductivity		x			
	θ_{w_v} [-]	Water content			x	x	
	α_{T_v} [L]	Transversal dispersivity			x		
	$D_{a\_v\,i}$ [L^2/T]	Free diffusion coefficient in air of the ith compound			x	x	
	$K_{H\,i}$ [-]	Dimensionless Henry's law constant of the ith compound			x	x	
	R_2 [L]	Radial distance from the center of the source at which the concentrations are expected to be zero (for non-degradable compounds only)				x	
	B_f [L]	Thickness of the capillary fringe				x	
Horizontal model	B [L]	Thickness of the aquifer	x	x	x	x	x
	u [L/T]	Groundwater velocity	x	x	x	x	x
	k_i [T^{-1}]	First order degradation rate	x	x	x	x	x
	n [-]	Porosity	x	x	x	x	x
	α_L, α_T, α_V [L]	Longitudinal (x), transverse (y) and vertical (z) dispersivity	x	x	x	x	x
	I_R [L/T]	Recharge over the aquifer	x	x	x**	x**	x

* in *Model V*: $C_1 = C_0$

** in *Model III*: $I_R = I$; in *Model IV*: $I = I_R = 0$

2.5 Horizontal transport models

Horizontal transport in the aquifer is calculated both in 2D and 3D. The 3D solution was developed for semi-infinite aquifers (there is no bottom of the aquifer) and determines the vertical (the z model direction) distribution of concentrations in the aquifer, including the effect of recharge over the aquifer that causes a downward migration and an increase of vertical dispersion and dilution of the plume as it is transported downstream in the aquifer. The inclusion of recharge results in a sinking of the plume, so that the maximum concentration does not always occur at the top of the aquifer, which would be unrealistic. The 2D model was developed for the case of 'thin' aquifers where the bottom boundary of the aquifer physically limits vertical transport processes. It is not easy to define when the aquifer is 'thin'; therefore both models are applied and the solution providing the most conservative (highest) concentration should be used.

An alternative could have been to use the 3D analytical solution with an impermeable boundary at the bottom of the aquifer located at $z=-B$. Such solutions are presented by Fischer (1979) and Wexler (1992). However, these solutions do not include recharge over the aquifer and so were not employed here.

The 3D advection-dispersion equation for horizontal transport with a uniform velocity u in the x-direction is:

$$R\frac{\partial c}{\partial t}+u\frac{\partial c}{\partial x}-D_x\frac{\partial^2 c}{\partial x^2}-D_y\frac{\partial^2 c}{\partial y^2}-D_z\frac{\partial^2 c}{\partial z^2}+kc=0 \qquad (1)$$

where R is the retardation factor [-]; c is the aqueous phase concentration [M/L^3]; u is the velocity in the x direction [L/T]; D_x, D_y and D_z are the directional hydrodynamic dispersion coefficients [L^2/T]; and k is the first order degradation rate [T^{-1}]. The boundary conditions are zero concentration $c(x,y,z=\infty)=0$ and zero gradients $\nabla c=0$ at an infinite distance from the point source.

The steady state solution to equation (1) for a point source was provided by Wexler (1992) (his equation 105 with $t\rightarrow\infty$). See also Hunt (1978) (equation 12) and the USEPA software Plume3D (Wagner et al., 1985). With a contaminant source area at the top of the aquifer of

$L_xL_y = \left(0 < X_c < L_x, -\frac{L_y}{2} < Y_c < \frac{L_y}{2}\right)$ at $z=0$ with concentration C_1 and infiltration rate I, the point source solution can be integrated over the area L_xL_y to obtain:

$$c(x,y,z)=\int_{-L_y/2}^{L_y/2}\int_{0}^{L_x}\frac{C_1 I}{4\pi n\gamma\sqrt{D_yD_z}}\left\{\exp\left(\frac{u(x-X_c)}{2D_x}-\frac{\beta\gamma}{2D_x}\right)\right\}dX_c\,dY_c \qquad (2)$$

where:

$$\beta = \left(u^2 + 4D_x k\right)^{1/2}$$

$$\gamma^2 = \left(x - X_c\right)^2 + \frac{D_x}{D_y}\left(y - Y_c\right)^2 + \frac{D_x}{D_z} z^2$$

$$D_x = \alpha_L u$$

$$D_y = \alpha_T u$$

$$D_z = \alpha_V u$$

In Eq. (2) C_I is the concentration at the top of the aquifer; Xc, Yc are the spatial coordinates of the contaminant point source [L]; Eq. (2) is only valid for $\gamma>0$. The solution can determine concentrations in the aquifer higher than those at source at small travel distances, because the point source is specified as mass discharge. Such concentrations are physically impossible, and so for $c > C_I$ the simulated concentration can be reset to $c = C_I$.

We include the effect of a homogeneous and constant (in time) recharge I_R over the top of the aquifer. The solution with recharge is obtained using the method of images (Fischer et al., 1979) assuming that aquifer recharge I_R [L/T] occurs only downstream of the source area. The assumption that the plume in the aquifer moves downward only downstream of the source is reasonable for contaminant sources that are small compared to the transport distances, but underestimates the vertical spreading of the plume for large sources, e.g. landfills. The method of images solution including the effect of groundwater recharge for a source located at the top of the aquifer is:

$c_{final}\left(x,y,z\right) = c\left(x,y,z-z_I\right) + c\left(x,y,z+z_I\right)$	(3)
where: $z_I = \begin{cases} \dfrac{I_R\left(x-L_x\right)}{nu} & x > L_x \\ 0 & x \le L_x \end{cases}$	

In Eq. (3) *c(x,y,z)* is the concentration obtained from Eq. (3). Eq. (2) shows that the plume sinks with constant downward velocity acting from *x* distances greater than the downstream edge of the source (note that *Model III* and *IV* have a different coordinate system and $x\text{-}L_x$ should be replaced by $x\text{-}L_x/2$).

Eq. (3) shows that the final concentration is found by shifting the source by $-z_I$ and adding an image source at z_I to simulate the top boundary condition. Since the solution is obtained by the method of images, it sets the boundary gradient to be $dc/dz=0$ at the top of the aquifer. The solution determines the correct contaminant mass balance, and when the plume has migrated away from the top boundary, the solution is exact. For contaminant plumes located near the top of the aquifer, the solution is only approximate, because the boundary condition $dc/dz=0$ only sets the dispersive flux at the boundary to be zero and neglects vertical advective downward transport at the boundary. The approximate solution was compared with a numerical model in Miljøstyrelsen (2016b) and was shown to be a reasonable approximation. The resulting concentrations in the aquifer are a little higher than those with a more appropriate zero total flux (dispersive and advective) at the boundary, but this is reasonable for risk assessment purposes.

In the case of no recharge, the image theory implies that concentrations in the half domain (the aquifer) are obtained by multiplying Eq. (2) by a factor of 2 (Fischer et al., 1979).

The 3D model can be used to compute mean concentrations over a well screen. This is done by averaging the simulated concentrations at discrete points along a specified well screen length. Typically, well screens are vertical (aligned with *z* direction) and have a length of few meters.

2D solutions can be used to simulate the horizontal transport of contaminants from sources in relatively thin aquifers, where the solute is generally well mixed throughout the thickness of the aquifer and vertical concentration gradients are negligible. Wexler et al. (1992) and Hunt (1978) provided a 2D steady-state semi-analytical solution for a point source located in a thin aquifer with uniform concentrations assumed in the *z* direction. In this case the boundary conditions applied are zero concentration $c(x,y,z=\infty)=0$ and zero gradients $\nabla z=0$ at infinite distance from the point source. The point source analytical solution can be integrated over the source area to obtain:

$$c(x,y)=\int_{-L_y/2}^{L_y/2}\int_{0}^{L_x}\frac{C_1 I\exp\left(\frac{u(x-X_C)}{2D_x}\right)}{2B\pi n\sqrt{D_xD_y}}K_o\left(\gamma\sqrt{\frac{u^2}{4D_x}+k}\right)dX_c dY_c \qquad (4)$$

where:

$$\gamma=\sqrt{\frac{(x-X_C)^2}{D_x}+\frac{(y-Y_C)^2}{D_y}}$$

In Eq. (4) *B* is the thickness of the aquifer [L] and K_0 is the modified Bessel function of second kind and zero order. Similar to Eq. (2) Eq. (4) is only valid for $\gamma>0$ and concentrations in the aquifer higher than those at the source can be obtained.

Eq. (2) and (4) are employed for *Model I, II* and *V*. *Model III* and *IV* have a non-homogeneous spatially distributed mass discharge per unit area [M/T/L^2] at the top of the aquifer $J(X_c,Y_c)$. Therefore, integration intervals are set at infinity, both in the 3D eq. (5) and the 2D eq. (6) solutions.

$$c(x,y,z)=\int_{-\infty}^{\infty}\int_{-\infty}^{\infty}\frac{J(X_c,Y_c)}{4\pi n\gamma\sqrt{D_yD_z}}\left\{\exp\left(\frac{u(x-X_c)}{2D_x}-\frac{\beta\gamma}{2D_x}\right)\right\}dX_c dY_c \qquad (5)$$

$$c(x,y)=\int_{-\infty}^{\infty}\int_{-\infty}^{\infty}\frac{J(X_c,Y_c)}{2B\pi n\sqrt{D_xD_y}}\exp\left(\frac{u(x-X_C)}{2D_x}\right)K_o\left(\gamma\sqrt{\frac{u^2}{4D_x}+k}\right)dX_c dY_c \qquad (6)$$

The mass discharge per unit area $J(X_c,Y_c)$ of *Model III* is given by the product of the infiltration rate *I* with the spatially distributed concentration at the top of the aquifer $C_1(X_c,Y_c)$ (output of the vertical model); whereas, the mass discharge of *Model IV* is computed using Fick's Law assuming that there is water diffusion through the capillary fringe:

$$J(X_c, Y_c) = \frac{C_1(r) D_w^e}{B_f} \qquad (7)$$

where:

$$r = \sqrt{X_c^{\ 2} \cdot Y_c^{\ 2}}$$

In Eq. (7) $C_1(r)$ is the concentration at the top of the aquifer that is the output of the vertical model [M/L^3]; D^e_w is the effective diffusion coefficient in water [L^2/T] and B_f is the thickness of the capillary fringe and r is the radial distance from the centre of the source (the vertical model is in polar coordinates).

The integrals can be solved numerically over finite integration intervals. An integration interval from – $10\ max(L_x,L_y)$ to $10\ max(L_x,L_y)$ for *Model III* and from $-150R_1$ to $150R_1$ (R_1 is the source radius) were found to be sufficient (Miljøstyrelsen, 2017) for most unsaturated zone thicknesses and air diffusion coefficients.

In *Model III* the infiltration at the source area I and the recharge over the aquifer I_R must be equal since the vertical model assumes a spatially uniform vertical velocity in the unsaturated zone. *Model IV* assumes no infiltration ($I=I_R=0$).

2.6 Vertical transport models

2.6.1 Model I. Vertical transport model within a saturated aquitard

Model I assumes that the aquitard is saturated (Figure 1) and so there is no air transport. The most significant transport processes within a homogeneous saturated aquitard are advection, diffusion and mechanical dispersion in the aqueous phase, and degradation. The aquitard can be saturated due to capillary rise in the low permeability material or because the piezometric head is above the source. The transport equation for *Model I* is similar to eq. (1) where only the vertical z direction is considered.

The 1D steady-state solution (van Genuchten et al., 1982) is shown in Eq. (8). This solution was found by applying the boundary conditions of fixed concentration at the source $c(0)=C_o$ and zero gradient at infinite distance from the source $\partial c/\partial z(\infty)=0$. The 1D solution provides similar results to a 3D solution in fully saturated conditions because dispersion processes in saturated vertical transport are negligible over short distances (Troldborg et al., 2008).

$$c(z) = C_0 \exp\left(\frac{(v-u_u)z}{2D_z}\right) \qquad (8)$$

where:

$$u_u = v\left(1 + \frac{4kD_z}{v^2}\right)^{1/2}$$

$$D_z = v\alpha_L + D_w^e$$

In Eq. (8) D_w^e is the effective diffusion coefficient in water [L^2/T]; c is the aqueous phase concentration [M/L^3]; v is the velocity in the z direction [L/T]; D_z is the hydrodynamic dispersion in water [L^2/T]; k is the first order degradation rate [T^{-1}] and α_L is the longitudinal dispersivity in water.

2.6.2 Model II. Vertical transport model within a saturated fractured clay

The vertical transport model of *Model II* simulates the downward vertical contaminant transport in a saturated fractured aquitard from the source to the top of the underlying aquifer. The contaminant transport is controlled by advection in the fractures and diffusion in the matrix (Chambon et al., 2011). The contaminant flux from the source is transported through vertical (equally distanced) parallel fractures separated by a distance *2B* and with fracture thickness (aperture) of 2b.

Several different mathematical models describing the contaminant transport in fractured clayey tills are described by Chambon et al. (2011). *Model II* employs the model with a constant source concentration. The mathematical model is based on the following assumptions (in addition to those already mentioned in Section 2.2): mass transport along the fracture is one-dimensional; dispersion along the fracture is neglected; advection in the porous matrix is neglected; transport in the matrix is perpendicular to the fracture. This approximation is reasonable if the hydraulic conductivity of the matrix is low compared to the hydraulic conductivity of fractures.

Applying a boundary condition of zero concentration at infinite distance from the source $C_f(\infty,t)=0,$ the steady-state solution becomes (Chambon et al., 2011):

$C_f(z) = C_0 \exp\left(-\frac{kz}{v_f}\right)\exp\left(-\frac{nz\sqrt{D_m k}}{v_f b}\right)$	(9)
where: $D_m = \tau D_w$	

In Eq. (9) z is the distance from the source [L]; v_f is the water velocity in the z direction of the fracture [L/T]; D_m is the effective diffusion coefficient in the water in the matrix [L^2/T]; D_w is the free diffusion coefficient in water [L^2/T]; n is the matrix porosity [-]; τ the matrix tortuosity [-]; and b is the half aperture of the fracture [L]. The effective diffusion coefficient was calculated according to Bear (1972) and tortuosity can be assumed equal to the matrix porosity n as a first approximation (Parker et al., 1994).

The water velocity in the fractures v_f is calculated using the cubic law (Snow, 1969); see Eq. (10). Assuming that the hydraulic conductivity for the clay matrix is very low (generally $< 10^{-9}$ m/s, Jørgensen et al., 2002), the average fracture aperture $2b$ can be calculated from the bulk hydraulic conductivity K_b and the spacing between two vertical fractures $2B$ (Mckay et al. 1993). Eq. (10) is a system of 3 equations with 5 parameters (K_b, $2b$, $2B$, I and i); therefore, only 3 must be defined in order to ensure physical consistency between the 5 parameters (Chambon et al., 2011):

$$v_f = (2b)^2 \frac{\rho g}{12\mu} i \qquad (10)$$

where:

$$2b = \left(K_b 2B \frac{12\mu}{\rho g} \right)^{1/3}$$

$$K_b = \frac{I}{i}$$

In Eq. (10) ρ is the density of water [M/L^3]; g is the gravitational acceleration [L/T^2]; μ is the kinematic viscosity of water; i is the hydraulic gradient and K_b is the bulk hydraulic conductivity [L/T]. It is recommended to specify the infiltration rate at the source I; the spacing between the fractures *2B;* and either the bulk hydraulic conductivity K_b or the fracture aperture *2b*.

There are some limitations to the vertical fractured model (Chambon et al., 2011): (1) the tool is not suitable for highly fractured media, with small average fracture spacing ($2B < 1\text{-}1.5\ m$) (an equivalent porous media model, such as *Model I*, can be used for fracture spacing of less than 0.40 m); (2) the validity of the single fracture assumption is controlled by the diffusion time from the fracture to the middle of the porous matrix, which can be characterized by $R_m B^2/D_m$ (R_m= retardation factor on the matrix; B= half spacing between fractures; D_m= effective diffusion coefficient in water in the matrix). If this diffusion time is large compared to the leaching time considered (the ratio between the vertical transport distance and the velocity in the fracture), the assumption of single fracture is reasonable (otherwise, an equivalent porous media model such as *Model I* can be used); (3) diffusion is assumed to be the dominant process in the porous matrix, so the model is applicable to low-permeability deposits only (such as clayey tills); (4) some studies show that degradation occurs preferentially in and around high permeability zones especially when the transport of bacteria, reactants or nutrients is limited by diffusion (Hønning et al., 2007; Scheutz et al., 2010) and/or by pore size exclusion (Lima et al., 2007). In such case the attenuation due to degradation can be overestimated by *Model II* since it assumes degradation both in the fractures and in the matrix.

2.6.3 Model III. Vertical transport model in the unsaturated zone

Model III simulates vertical transport in the unsaturated zone below the source. The model was presented by Troldborg et al. (2009) and includes the processes of advection and dispersion in the aqueous phase, diffusion in the air phase and degradation. Studies have shown that diffusion in the air phase is a dominant transport process in the unsaturated zone, particularly for volatile compounds (Christophersen et al., 2005). Both field data and model results show that the risk of groundwater contamination from volatile compounds is limited in areas in contact with the atmosphere due to diffusive transport (Lahvis et al., 2004; Grathwohl et al., 2002).

By coupling the transport equations for water and air and employing the phase partitioning expression $C_a = K_H \cdot C_w$, the transport equation Eq. (11) is obtained (Troldborg at al., 2009).

$\frac{\partial (R\theta_w + K_H \theta_a) C_w}{\partial t} = \nabla(\theta_w \mathsf{D}_w + \theta_a K_H \mathsf{D}_a)\nabla C_w - I\frac{\partial C_w}{\partial z} - \theta_w k C_w$	(11)

where R is the retardation factor [-]; C_w is the aqueous phase concentration [M/L^3]; K_H is the dimensionless Henry's law constant [-]; θ_a is the air content [-] and D_w and D_a are dispersion tensors in water and air [L^2/T].

The 3D steady-state solution of *Model III* with boundary and initial conditions describing a source of concentration C_0 perpendicular to the flow direction ($C_w(x,y,z=0,t)=C_0$ at $-L_x/2<x<L_x/2$ and $-L_y/2<y<L_y/2$; $C_w(x,y, z=0,t)=0$ otherwise) is (Troldborg et al., 2009):

$$C_w(z,x,y) = \frac{C_0}{8}\int_{\tau=0}^{\tau=\infty} f_z^{'}(z,\tau) f_x^{'}(x,\tau) f_y^{'}(y,\tau)\, d\tau \qquad (12)$$

where:

$$f_z^{'}(z,\tau) = \frac{z}{\sqrt{\pi D_z}} \exp\left(\frac{vz}{2D_z}\right) \cdot \exp\left[-\tau\left(\frac{v^2}{4D_z} + k'\right) - \frac{z^2}{4D_z\tau}\right] \cdot \tau^{-3/2}$$

$$f_x^{'}(x,\tau) = \left\{ erf\left[\frac{x+\frac{L_x}{2}}{2\sqrt{D_x\tau}}\right] - erf\left[\frac{x-\frac{L_x}{2}}{2\sqrt{D_x\tau}}\right]\right\}$$

$$f_y^{'}(y,\tau) = \left\{ erf\left[\frac{y+\frac{L_y}{2}}{2\sqrt{D_y\tau}}\right] - erf\left[\frac{y-\frac{L_y}{2}}{2\sqrt{D_y\tau}}\right]\right\}$$

$$v = \frac{I}{\theta_w}$$

$$k' = \theta_w k$$

$$D_x = D_y = \theta_w \alpha_T v + \theta_w D_w^e + \theta_a D_a^e K_H$$

$$D_z = \theta_w \alpha_L v + \theta_w D_w^e + \theta_a D_a^e K_H$$

$$D_a^e = D_a \frac{\theta_a^{1.5}}{n}$$

$$D_w^e = 10^{-4} D_a^e$$

In Eq. (12) v is the pore water velocity in the z direction [L/T]; D_a^e and D_w^e are the effective diffusion coefficients in air and water [L^2/T] and D_a is the free diffusion coefficient in air [L^2/T].

2.6.4 Model IV. Vertical transport model in the unsaturated zone without infiltration

In *Model IV*, the main transport process is the air diffusion in the horizontal direction of the unsaturated zone. Eq. (13) (Troldborg et al., 2009) shows the transport equation for volatile and reactive contaminants formulated in radial coordinates when there is zero water advection.

$$\frac{\partial(R\theta_w + K_H\theta_a)C_w}{\partial t} = (\theta_a K_H D_a^e + \theta_w D_w^e)\left(\frac{\partial^2 C_w}{\partial r^2} + \frac{1}{r}\frac{\partial C_w}{\partial r}\right) - \theta_w k C_w \qquad (13)$$

where R is the retardation factor [-]; C_w is the aqueous phase concentration [M/L^3]; θ_a is the air content [-]; t is the time; D_w^e and D_a^e are the effective dispersion coefficient in water and air [L^2/T] respectively and r is the radial distance from the center of the source [L].

With the boundary conditions $C_w(0<r<R_1)=C_0$ (R_1 is the source radius) and $C_w(r\to\infty)=0$, the steady-state solution for degradable compounds was given by Spiegel (1968):

$$C_w(r)=\frac{C_0}{K_0(R_1\omega)}K_0(r\omega) \qquad (14)$$

where:

$$\omega=\sqrt{\frac{\theta_w\lambda}{\theta_a K_H D_a^e+\theta_w D_w^e}}$$

In Eq.(14) K_0 is the modified Bessel function of second kind and order 0 and R_1 is the source radius [L].

Similarly the steady-state solution for non-degradable compounds was given by Luikov and Hartnett (1968):

$$C_w(r)=\frac{C_0}{\ln\left(\frac{R_2}{R_1}\right)}\ln\left(\frac{R_2}{r}\right) \qquad (15)$$

where R_2 is the radial distance at which the concentration is set to zero. This distance can be physically interpreted as the distance at which the terrain surface is no longer covered by an impervious area and therefore air diffusion to the atmosphere occurs.

2.7 Coupling between the vertical and horizontal transport models

The vertical and horizontal transport models are coupled in a similar way for *Model I*, *II*, *III* and *IV* (see Figures 1 to 4; *Model V* does not have a vertical model embedded). The different vertical transport models compute the concentration at the top of the aquifer C_1 (at a vertical distance Z_v from the source) that is used to compute the spatially distributed mass discharge input to the horizontal models.

In *Model I* and *II*, C_1 is assumed to be uniformly distributed over the source area L_xL_y. This is reasonable because lateral dispersion processes are small in aquitards and fractured clays. Moreover, the diffusive flux from the clay interface at the bottom of the aquitard into the aquifer is small and so it is not considered. In *Model II*, the assumption of fully mixed conditions at the bottom of the fractures might result in a small (but acceptable) underestimation of the contaminant concentration at a point of compliance in the aquifer (Miljøstyrelsen, 2017). The uniformly distributed mass discharge for the horizontal model is obtained by integrating over the source area L_xL_y the product of the concentration C_1 and the water infiltration rate I as shown in Eq. (2) and Eq. (4).

In *Model III* and *IV*, $C_1(x,y)$ is spatially distributed over the top of the aquifer because gas transport contributes to significant lateral dispersion. The spatially distributed mass discharge to the aquifer in *Model III* is obtained by integrating over the top of the aquifer the product of the concentration $C_1(x,y)$ and the water infiltration rate I as shown in Eq. (5). The mass discharge to the aquifer in *Model IV* is computed using Fick's law because water diffusion across the capillary fringe is assumed to occur (there is zero vertical water advection due to the impervious areas above the source). The spatially distributed mass discharge to the aquifer in *Model IV* is obtained by integrating over the top of the aquifer the spatially distributed water diffusion flux per unit area as shown in Eq. (7).

2.8 Sequential degradation model

Reactive processes were included in the models using the approach of Sun et al. (1999a, 1999b), who determined the concentrations of compounds in a degradation chain. The method is easy to implement and only the degradation rates k_i and stoichiometric ratios Y_i can be varied for each of the individual compounds. The sequential model is expected to be used mainly for chlorinated ethenes undergoing reductive dechlorination under anaerobic conditions (Chambon et al., 2013). In *Model III* and *IV*, we simulate spreading in the unsaturated zone using different parameters for each compound of the degradation chain. Here aerobic conditions are most likely, so exclusion of sequential degradation is a minor issue for practical purposes, and this is why we did not include sequential degradation in *Models III* and *IV*.

The solution approach consists of three steps. The first step is to define a set of auxiliary variables a_i for each compound of the degradation chain:

$$a_i = \begin{cases} c_i & i=1 \\ c_i + \sum_{j=1}^{i-1}\left(\prod_{l=j}^{i-1}\frac{Y_{l+1}k_l}{k_l-k_i}\right)c_j & i=2,3,....,n \end{cases} \qquad (16)$$

where c_i is concentration of the i^{th} compound resulting from the semi-analytical models presented above; Y is the stoichiometric molar mass ratio of sequential compounds (M_{i+1}/M_i) (the first element of the degradation chain has $Y_1=1$) and k is the first-order degradation rate. The introduction of the auxiliary variables decouples the governing equations for the compounds. In the second step, the governing equations are solved for the auxiliary variables a_i. The third step then determines the final concentrations according to:

$$c_i = \begin{cases} a_i & i=1 \\ a_i - \sum_{j=1}^{i-1}\left(\prod_{l=j}^{i-1}\frac{Y_{l+1}k_l}{k_l-k_i}\right)c_j & i=2,3,....,n \end{cases} \qquad (17)$$

2.9 Computer coding, implementation and application

All models were implemented in MATLAB by the authors. They are currently being recoded for insertion into a single graphical user interface, which will be made available online by the Danish EPA. Model run times are instantaneous for point evaluations of *Models I, II* and *IV*, and up to tens of seconds for *Models III* and *IV*. Graphical output of the spatial variability of concentrations requires more time. Short run times are essential as the tool is intended to be used for the assessment of many thousands of sites.

Model I and *V* are currently being used in a risk assessment framework (developed in collaboration with the Danish EPA) that aims at ranking and identifying critical contaminated sites in Denmark. In this framework, *Model I* and *V* were used to simulate thousands of sites of the national database (with more than 35,000 sites). The database includes information (including all the parameters needed to run the transport models) describing each contaminated site. In this framework, uncertainty was addressed by examining several scenarios with different parameters and model conceptualizations; and both contaminant mass discharge over a control plane and concentrations at a control point were examined to determine risk.

3. Results

The tool was applied to two different case studies in Denmark in order to illustrate the applicability in a preliminary risk assessment context. The model parameters used in the case studies were chosen either from literature or from site specific data and with the aim of providing conservative estimates; however, this can be difficult because some parameters are inversely correlated. For example, high groundwater velocities enhance dilution and spreading, but result in small degradation due to short travel times. It should be noted that the model parameters are uncertain because of limited data availability at the two sites, even though these two cases are very well characterized compared to the great majority of the thousands of contaminated sites in Denmark. Hence, parameter uncertainty will always be a major concern in contaminant site risk assessment applications.

Sensitivity and uncertainty analysis, calibration, and validation of the models are beyond the scope of this study, because it is focused on the development of tools for an early stage risk assessment of contaminated sites. These subsequent modelling steps are part of a more detailed contaminated site analysis, where the most critical sites are to be identified and the risk re-evaluated.

For each site the two most representative model conceptualizations among the five transport models are selected. Two conceptualizations are employed because both sites deal with non-aqueous phase liquids and so the source could have migrated downward to the aquifer. In this way we show how uncertainty in the transport conceptualization can be addressed.

The results from the simulations are also compared with groundwater concentration data from the two sites. Objective of the comparison is only to qualitatively discuss whether a first and conservative parameter selection would actually produce a conservative estimation of aquifer contaminations useful for a first screening/assessment. Observation data are also sparse and so data from different years and different sampling campaigns are often combined, making comparison difficult.

Results are only shown for depth averaged concentrations over a 1 m long screen, even though the models provide contaminant mass discharge as well.

3.1 Case study 1. Risk assessment application of *Model I* and *V*

Models I and *V* are applied to a contaminated site where chlorinated solvents were used at a machine factory operating in the period 1951-1989. The site description and the observation data used in the calculations are based on published site characterization reports and two scientific papers (Jørgensen, 2003, 2007a and 2007b; Scheutz, 2008 and 2010). The site investigations carried out before 2003 showed high concentrations of cis-dichloroethylene (cis-DCE) and its degradation product vinyl-chloride (VC). The main substance that leaked from an underground storage tank was trichloroethylene (TCE). The exact period of leakage is unknown. Site investigations showed that TCE concentrations downstream of the tank were small, mainly due to its almost complete degradation to cis-DCE and VC.

Figure 6 shows a sketch of the geology and contamination distribution at the site. Two scenarios are simulated with different source locations. The first uses *Model I* where the source is assumed to be within the saturated clay layer located above the aquifer (both vertical and horizontal transport); the second uses *Model V* where the source is assumed to be in contact with the aquifer (only horizontal transport) after the non-aqueous phase liquids migrated downward from the original source.

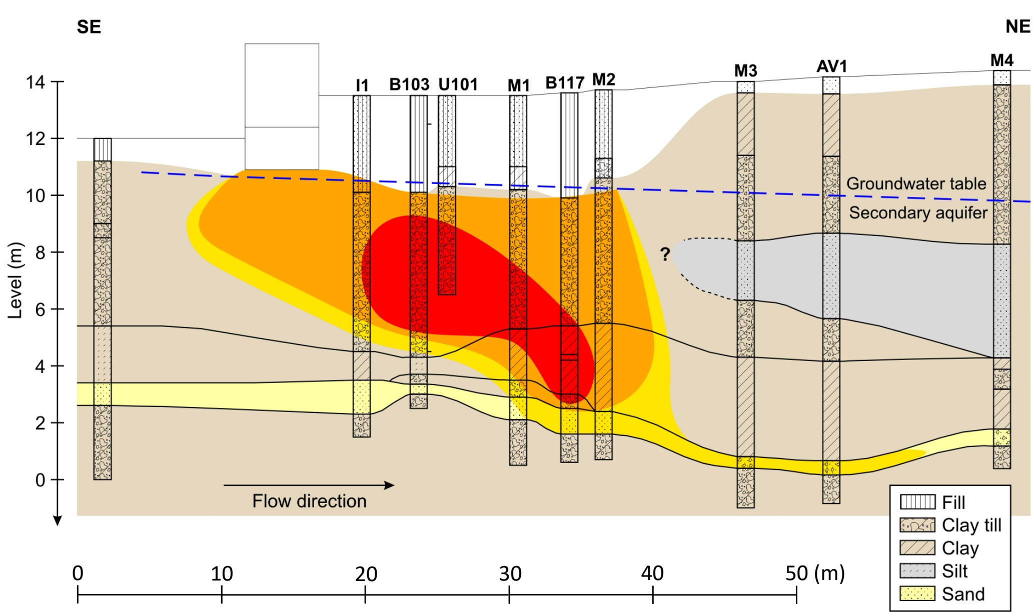

Figure 6. Sketch of *Case study 1*. Cross section showing the geology in the groundwater flow direction, some investigation wells, the confined sandy aquifer, the water table, and an estimate of the extent of contamination (red=high; orange=medium; yellow=low concentrations).

The bottom of the leaking tank is located 2 m below the ground surface, within a saturated clay layer that extends 9-12 m below terrain. Below the clay layer, a 1 m thick sandy aquifer flows with a mean annual groundwater velocity of about 126 m/y. The piezometric head in the clay is higher than in the underlying aquifer and so a vertical downward water flow is expected.

The highest concentrations at the time of the site investigations were found to be 2-6 m below the leaking tank and 5-25 m away from it (there had been horizontal transport in the clay layer likely due to the presence of sand lenses). The model source area is estimated to be 30 x 10 m^2 ($L_x \cdot L_y$). The highest concentrations in the area of both cis-DCE (240 mg/L) and VC (25 mg/L) were found at a well with a screen depth from 6 to 7 m below terrain level and are used as model inputs (see Table 4) (The threshold concentrations of cis-DCE and VC for drinking water standards are typically on the order of few µg/L). The mean annual net infiltration in the area was estimated to be 100 mm/y. The annual contaminant mass discharge can be estimated by multiplying the source area by the annual net infiltration and the input concentration. The contaminant discharge is therefore 7.2 kg/y for cis-DCE and 0.75 kg/y for VC. Table 4 shows the model parameters that were used in the simulations.

Table 4. Parameters of Case study 1. Risk assessment application of *Model I* (vertical and horizontal transport) and *Model V* (horizontal transport).

Parameter	Description	Value	Reference
Global inputs			
Y	Stoichiometric ratio VC- DCE	0.648 [a)]	
I	Source infiltration rate	100 mm/y	Jørgensen et al. (2007b)
L_x	Source length	30 m [b)]	
L_y	Source width	10 m [b)]	
Co_{DCE}	Concentration of DCE	240 mg/L	Jørgensen et al. (2007a)
Co_{VC}	Concentration of VC	25 mg/L	Jørgensen et al. (2007a)
Vertical transport inputs			
$k_{\_v}$	First order degradation rate of DCE	0.00016 day^{-1}	Wiedemeier et al. (1997)
	First order degradation rate of VC	0.0003 day^{-1}	Wiedemeier et al. (1997)
n_{v}	Porosity of clay	0.35	
α_{L_v}	Longitudinal dispersivity (z direction)	0.1 m	Vanderborght and Vereecken (2007)
$Z_{\_v}$	Distance between the bottom of the source and the top of the aquifer	5 m	
D_{w_v}	Free diffusion coefficient in water of DCE	$1.13 \cdot 10^{-9}$ m^2/sec	US EPA (1996)
Horizontal transport inputs			
I_R	Groundwater recharge	100 mm/y [c)]	
B	Thickness of the aquifer	1 m [d)]	
u	Groundwater velocity	126 m/y [e)]	
k	First order degradation rate of DCE	0.00016 day^{-1}	Wiedemeier et al. (1997)
	First order degradation rate of VC	0.0003 day^{-1}	Wiedemeier et al. (1997)
n	Porosity of sand	0.25	
α_L	Longitudinal dispersivity (x)	1 m [f)]	
α_T	Transversal dispersivity (y)	0.01 m [f)]	
α_V	Vertical dispersivity (z)	0.005 m [f)]	

[a)] Ratio of molar masses: $Y_{VC\text{-}DCE}$ = (62.5 g/mol) / (96.4 g/mol)
[b)] Assessed from soil and water concentrations found from site descriptions in Jørgensen et al. (2007a; 2007b)
[c)] Assumed to be the same as I
[d)] Assessed from site descriptions in Jørgensen et al. (2007a; 2007b)
[e)] Assessed from site description in Jørgensen et al. (2007a; 2007b) using Darcy's Law
[f)] Chosen from an interval found from a literature review (Chiang et al., 1989; Mallants et al., 2000;

Rivett et al., 1994; Robertson et al, 1991; Rotaru et al., 2014; Schulze-Makuch, 2005). Intervals are: α_L 0,2-1 m, α_T 0,0025-0,3 m, and α_V 0,008-0,01 m.

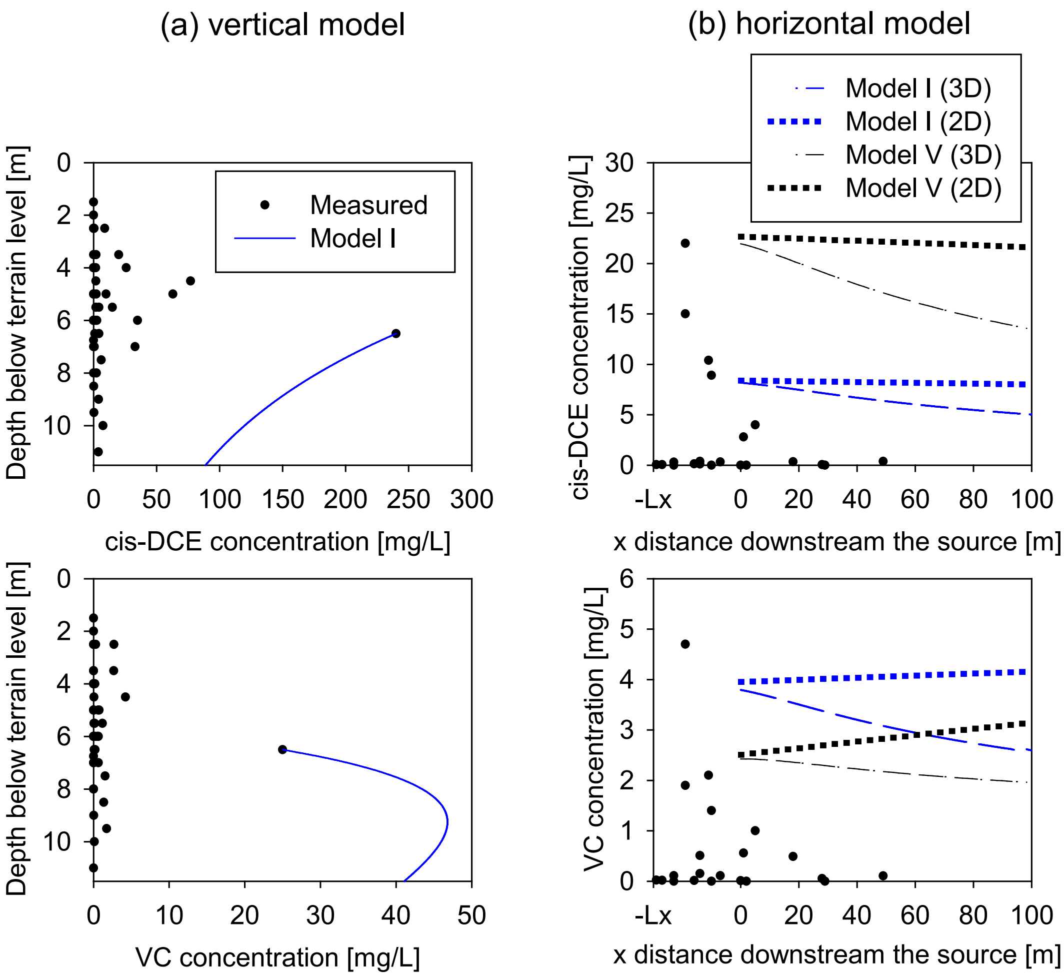

Figure 7. cis-DCE and VC model results for case study 1. (a) Vertical model results and observed aqueous phase concentrations in the clay layer overlying the aquifer at 11.5 m depth. (b) 3D and 2D horizontal model results and observed aqueous phase concentrations in the aquifer. The simulated source area is located between *–Lx* and *0* m of the x axis.

Figure 7a shows the vertical model results and the observed concentrations. The observed concentrations measured between the surface and the top of the aquifer (11.5 mbs), include both pore water and soil phase concentrations. The solid phase concentrations were converted into aqueous phase concentrations using partitioning coefficients K_d (determined by laboratory experiments with sediments from the site) of 0.78 kg/L for cis-DCE and 0.29 kg/L for VC (Lu et al., 2011). The contaminant source in *Model I* was assumed to be located at 6.5 m below terrain level (in correspondence to the level at which maximum concentrations were observed) and in *Model V* at the top of the aquifer. The simulated cis-DCE concentrations are shown to decrease with depth from the source. The decreasing cis-DCE simulated concentration patterns are qualitatively similar to the observations, but the simulated concentrations are significantly higher. This is because the model input concentration was based on the highest cis-DCE observed concentration (a value of 240 mg/L, well above all other observations).

The simulated VC concentrations are shown to initially increase and then decrease downstream of the source. The modelled increase in VC with depth is due to the degradation of cis-DCE into VC. The VC simulated concentration patterns and values do not match the observations, the latter being significantly lower, because the model input concentration is based on the highest observed VC concentration (25 mg/L), again significantly larger than all other observations values.

Figure 7b shows the horizontal model results and the observed data. The simulated concentrations are mean values over a well screen of 1 m length (the aquifer is 1 m thick) located at the centerline of the plume. Both the 2D and 3D horizontal transport model results are shown and the model determining the highest concentrations would typically be chosen for risk assessment purposes. Both the observed and simulated concentrations of cis-DCE and VC in the aquifer show similar patterns for both models: the observed concentrations show a peak below the source area (between $-Lx$ and *0* of the x axis), and then a decrease with increasing distance downstream in the aquifer; the 3D models shows a decreasing pattern downstream the source, while the 2D models provides an almost constant concentration. The relatively constant concentration predicted by the 2D model is due to degradation being small because of the high groundwater velocity and the low degradation coefficients, combined with the fact that the aquifer is thin and transverse and vertical dispersivities do not have a significant effect. The 2D models of VC shows a trend of increasing concentration with distance that is due to degradation of cis-DCE into VC. The 3D model assumes an infinite aquifer in the vertical, so that the contaminant can spread without limitation in the *z*-direction. Instead, the 2D model assumes that there is a no flux boundary at the bottom of the aquifer and that concentrations are uniformly mixed over the full thickness. *Model I* and *V* show similar trends, but the concentrations immediately downstream the source are different due to the different source locations. It is interesting to note that *Model I* (vertical and horizontal transport) shows higher concentrations of *VC* compared to *Model V* (only horizontal transport); this occurs because the inclusion of vertical transport allows more time for cis-DCE to degrade into VC.

The placement of the uniformly distributed source area is uncertain in the *x* direction and the data suggests that the source could be shifted few tens of meters upstream or that the concentration in the source area might not be uniform. This uncertainty of source location is not modelled in this case study, but may explain some deviations between modelled and observed trends.

3.2 Case study 2. Risk assessment application of *Model III* and *V*

Models III and *V* are applied to a contaminated site where a dry-cleaning shop using chlorinated solvents operated in the period 1963-1998. PCE was used in the period 1980-1998, and other solvents may have been used before 1980. The description of the site and the observation data used in the calculations are based on published and unpublished site characterization reports and scientific papers (Københavns Amt, 2000, 2001a, 2001b; Christensen et al., 2002). The site investigations that were carried out in 1997-2001 showed high concentrations of PCE and TCE.

Figure 8 shows a sketch of the site geology and contaminant distribution. Two scenarios are simulated: the first one uses *Model III* as the source is assumed to be within the unsaturated sand layer above the aquifer (both vertical and horizontal transport); the second uses *Model V* as the source is assumed to be in contact with the aquifer (only horizontal transport) after the non-aqueous phase liquids migrated downward from the original source.

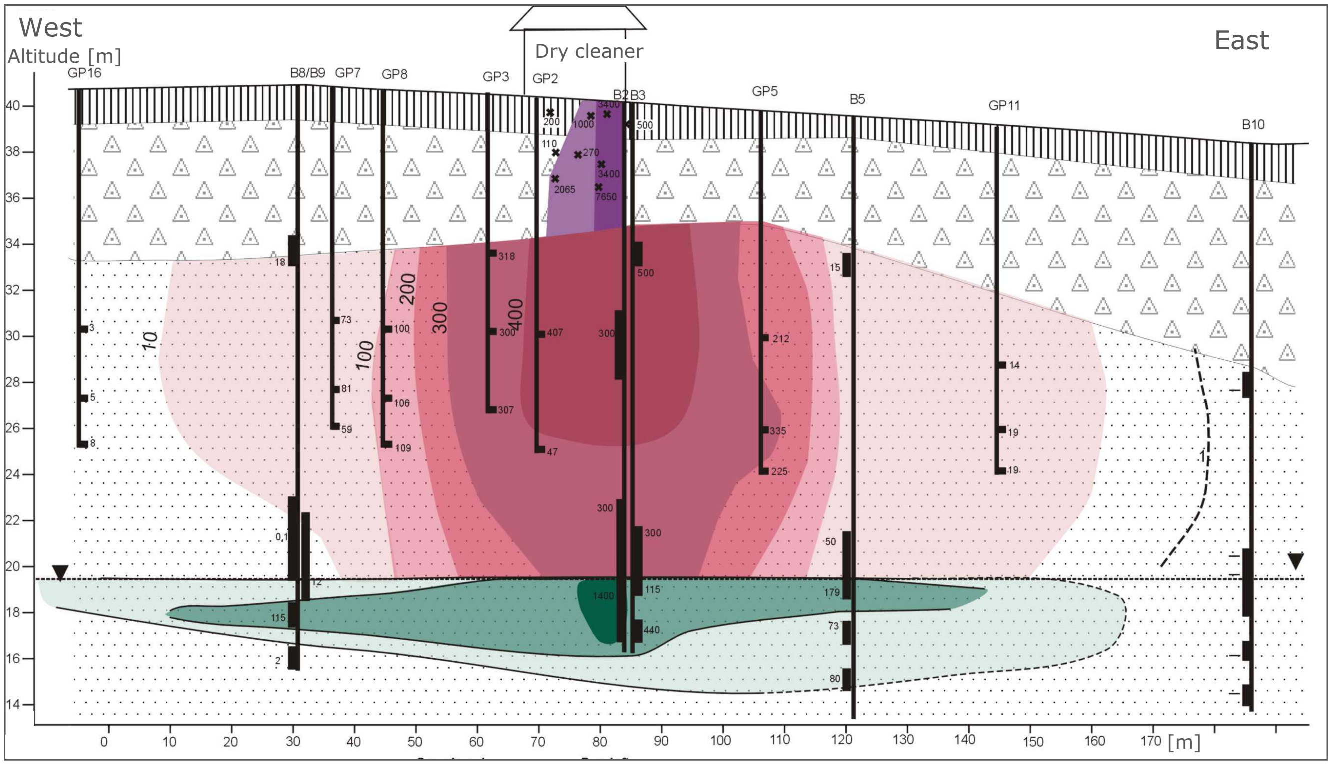

Figure 8. Sketch of *Case study 2*. Cross section showing the geology, the dry-cleaning shop, some investigation wells, the unconfined aquifer and the results of a previous study of the contaminant spreading (concentrations: violet=clay layer; red=unsaturated sand layer; green=aquifer). Figure from Københavns Amt (2000). Concentrations are shown in µg/L.

The main origin of the spill is likely to be a sewer manhole located just outside the dry-cleaning shop. The spill occurred within an unsaturated clay layer that extends down to about a depth of 5 m. A 16 m thick unsaturated sandy layer (down to -21 m) is located below the clay layer. The groundwater pollution is assessed for a 9 m thick unconfined sandy aquifer below the unsaturated sand, with a groundwater flow that significantly varies in both velocity and flow direction throughout the year. The mean annual groundwater velocity used in this case study is 35 m/y (direction north-west) and the annual infiltration rate is 161 mm/y based on the water resource model of Denmark (Højberg et al., 2015).

The area with the highest PCE concentrations (588 µg/L) at the time of the site investigations was found at approximately 10-11 m below surface in the unsaturated sandy layer. The area with the highest TCE concentrations (530 µg/L) was found 29-30 m below surface, close to the bottom of the unconfined sandy aquifer and approximately 20 m away (south-west) of the shop. The contaminant source area for *Model III* is estimated to be 25 x 15 m^2 ($L_x \cdot L_y$), assumed to be equal for both PCE and TCE even though the location of the PCE source area can be assumed to be 10.5 m below surface (in correspondence with the location of the highest concentration measurement) and the location of the TCE source area is right above the groundwater table. The simulated annual contaminant mass discharge from the source (calculated by multiplying the source area by the annual infiltration rate and the input concentration) is 36 g/y of PCE and 32 g/y of TCE.

Table 5 shows the model parameters. Note that only PCE parameters are defined for the vertical transport model since the TCE source was assumed to be at the top of the aquifer.

Table 5. Parameters of *Case study 2*. Risk assessment application of *Model III* and *V*.

Parameter	Description	Value	Reference
Source inputs			
Y	Stoichiometric ratio TCE- PCE	0.79 [a)]	
I	Source infiltration rate	161 mm/y	Højberg et al. (2015)
L_x	Source length	25 m [b)]	
L_y	Source width	15 m [b)]	
Co_{PCE}	Concentration of PCE	588 µg/L	Københavns Amt, (2001a and b)
Co_{TCE}	Concentration of TCE	530 µg/L	Københavns Amt, (2001a and b)
Vertical transport inputs			
k_{v}	First order degradation rate of PCE (aerobic)	0.0 day^{-1}	
n_{v}	Porosity of sand	0.25	
θ_{w_v}	Water content	0.10	Christensen et al. (2002)
α_{L_v}	Longitudinal dispersivity (z direction)	0.1 m	Vanderborght & Vereecken (2007)
α_{T_v}	Transversal dispersivity (z direction)	0.01 m	Troldborg et al. (2009)
$Z_{\_v}$	Distance between the bottom of the source and the top of the aquifer	10 m	
D_{a_v}	Free diffusion coefficient in air of PCE	$6.38 \cdot 10^{-6}$ m^2/sec	Lugg, G.A. (1968)
K_{H_v}	Dimensionless Henry's law constant of PCE	0.75	Troldborg et al. (2009)
Horizontal transport inputs			
I_{GW}	Groundwater recharge	161 mm/y [c)]	
B	Thickness of the aquifer	9 m	
u	Groundwater velocity	35 m/y	Højberg et al. (2015)
k	First order degradation rate of PCE (anaerobic)	0.00068 day^{-1}	Wiedemeier et al. (1997)
	First order degradation rate of TCE (anaerobic)	0.0001 day^{-1}	Wiedemeier et al. (1997)
n	Porosity of sand	0.25	
α_L	Longitudinal dispersivity (x)	1 m [d)]	
α_T	Transversal dispersivity (y)	0.01 m [d)]	
α_V	Vertical dispersivity (z)	0.005 m [d)]	

[a)] Ratio of molar masses: $Y_{TCE\text{-}PCE}$ = (131.4 g/mol) / (165.8 g/mol)
[b)] Assessed from the site descriptions in Københavns Amt (2001a; 2001b) and Christensen et al. (2002)
[c)] Assumed to be the same as I. It is recommended (see Section 2) that $I=I_R$ in Model III
[d)] Chosen from an interval found from a literature review (Chiang et al., 1989; Mallants et al., 2000; Rivett et al., 1994; Robertson et al, 1991; Rotaru et al., 2014; Schulze-Makuch, 2005). Intervals are: α_L 0,2-1 m, α_T 0,0025-0,3 m, and α_V 0,008-0,01 m.

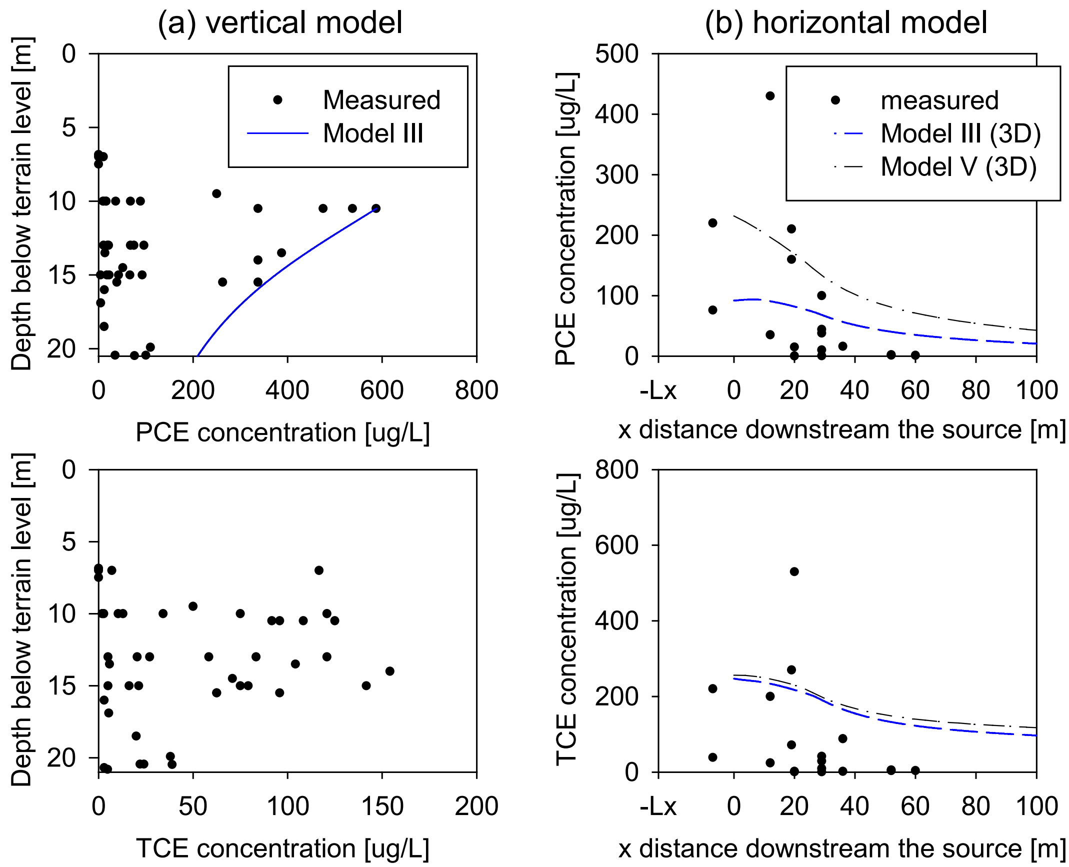

Figure 9. PCE and TCE model results of the *Model III* and *V* applications to the *Case study 2*. (a) Vertical model results and observed aqueous phase concentrations in the unsaturated sand layer where there is vertical downward transport up to the top of the aquifer at approximately 21 m below surface. TCE simulation results are not shown, as the source is assumed to be at the top of the aquifer. (b) 3D horizontal model results and observed aqueous phase concentrations in the aquifer along the flow direction. The simulated source area is located between –*Lx* and *0* m of the x axis.

Figure 9 shows the simulation results and the observed aqueous phase concentrations at the *Case study 2* site. Figure 9a shows the vertical model results and the observed concentrations. The observed concentrations in the unsaturated sand above the aquifer (located at 20.5 mbs), include both pore water and gaseous concentrations. The gaseous concentrations were converted into aqueous phase concentrations using the dimensionless Henry's law constants of 0.8 for PCE and 0.27 for TCE. The simulated PCE concentrations are shown to decrease with depth from the source. Both the simulated PCE concentration values and the decreasing concentration patterns are qualitatively in agreement with the observations. The TCE vertical transport model results are not shown, as the source was assumed to be at the top of the aquifer, so that only transport within the aquifer was simulated.

Figure 9b shows the horizontal model results and the observation data. The simulated concentrations are mean concentrations over a well screen of 1 m length located at the depth of maximum concentration. Only the 3D model results are shown since the 2D model resulted in significantly lower concentrations because it assumes that the contaminant is uniformly distributed over the 9 m thick aquifer. Both the observed and simulated concentrations of PCE and TCE in the aquifer (Figure 9b) show similar trends.

The simulated concentrations seem to be shifted horizontally 15-25 m in the x-direction compared to the observations. This means that the location of the simulated source might not be correct: the data suggests that it could be 15-25 m further downstream. However, conceptualization of the source location is not easy as the highest concentrations of PCE in the aquifer were found 10 m north-east of the dry-cleaning shop and the highest concentrations of PCE were found 20 m south-east. The decreasing trend of the observed concentrations is more pronounced compared to model results. This can be due to an underestimation of the simulated dispersion and degradation processes, and also the fact that the groundwater flow direction changes significantly throughout the year (different field campaigns show opposite flow directions), which might hinder the plume from travelling further from the source.

The simulated concentration in the aquifer is larger than the observed concentration for distances greater than 20 m downstream the source. The model overestimates aquifer concentrations as desired in risk assessment applications.

3.3 Discussion

The validity of risk assessment models is generally difficult to document because of the lack of appropriate observed data for comparison (Chambon et al., 2011). Although the measured field data did not fit well with the simulations, the model provides a first conservative estimate of contaminant concentrations in the aquifers affected by contaminated sites. Such estimates are valuable for risk assessment applications where thousands of sites must be assessed on the basis of poor data. Risk assessment applications are typically hampered by data limitations and input parameter uncertainties, and therefore they typically rely on simplified analytical models, with only the main transport processes, few model parameters, and conservative assumptions. These models are useful for an initial assessment of contaminant risk, for sensitivity and uncertainty analysis to determine the dominant transport processes involved, for scenario analysis, and for validating numerical solutions. A greater modeling effort (i.e. using numerical models) is not likely to provide more reliable results due to the scarcity of specific site data. An unrealistic amount of resources would be required to acquire the needed data for the thousands of sites which must be assessed.

The model outputs of risk assessment applications should be analyzed within the context of uncertainty of the model inputs, data limitation and the often necessary use of standard values from literature. Parameters typically vary significantly between different contaminated sites and within the same site. Some parameters can vary by several orders of magnitude, i.e. the degradation rates of a compound (Xu and Eckstein,1995; Troldborg et al., 2009; Verginelli and Baciocchi, 2013). The local groundwater velocity and flow direction can vary depending on seasonal recharge patterns or water abstraction from neighboring wells. Source zone contaminant mass discharge estimates can vary up to an order of magnitude for well characterized sites depending on the methods chosen, and can vary even more when data are scarce (Troldborg et al., 2012; Saha, et al., 2013). Dispersivity values in aquifers can also vary up to an order of magnitude and they are also dependent on the spatial scale of the processes (Gelhar et al., 1992; Schulze-Makuch, 2005). Dispersivity values in unsaturated and saturated zones are highly uncertain and few literature values are available (Vanderborght and Vereecken, 2007).

4. Conclusions

In this work, we examined tens of thousands of contaminated sites in Denmark and developed a tool consisting of five different semi-analytical contaminant transport models to provide conservative estimations of contaminant concentrations and mass discharge in aquifers downstream contaminated sites. The models provide conservative estimations that are useful for regulatory use when a large number of contaminated sites are to be assessed with limited data on geology, field observations, and with high parameter uncertainties. For instance the models can be used for ranking all the sites at national scale to then select those where resources should be allocated in the future for a further detailed assessment. The ensemble of the five different models is able to simulate typical scenarios encountered at contaminated sites; particularly, different source geometries with varying contaminant mass discharge, saturated/unsaturated zones with different geologies and volatile/non-volatile compounds. The comparison with observed data at two selected sites showed that the models can simulate the main trends and provide valuable information to assess the risk posed by contaminant sources to groundwater; particularly, the peak concentration, contaminant mass discharge and plume distribution at the point of compliance. In contrast, existing models struggle to adapt to such variety of practical conditions and might not provide all the outputs considered relevant for risk assessment. Finally, the models can also be used to predict the location of the center of the contaminant plume. This can be useful to determine sampling locations in monitoring campaigns that can support more advanced numerical models and implementation of remediation strategies. The models have recently been implemented by the Danish EPA as part of a national risk assessment framework.

Acknowledgements

This work was conducted as part of a project to develop a risk assessment tool for contaminated sites in Denmark and was supported by the Danish Environmental Protection Agency and the Technical University of Denmark. In particular we acknowledge the support from Jens Aabling, Danish EPA, during the development of the tool. Participants in end user workshops from Danish Regions, responsible for management of contaminated sites in Denmark, have contributed with valuable input to model needs and requirements.

REFERENCES

Andricevic, R., Cvetkovic, V., 1996. Evaluation of risk from contaminants migrating by groundwater. Water Resources Research, Vol. 32, No. 3, 611-621.

ANPA, 2002. ROME: ReasOnable Maximum Exposure - Operating Manual. National Agency for Protection of the Environment (Agenzia Nazionale Protezione Ambiente).

Aziz, C.E., Newell, C.J., Gonzales, J.R., 2000. BIOCHLOR – Natural Attenuation Decision Support System. User's Manual Version 1.0. US Environmental Protection Agency. US Environmental Protection Agency.

Bardos, P., Lewis, A., Nortcliff, S., Matiotti, C., Marot, F., Sullivan, T., 2002. Review of Decision Support Tools for Contaminated Land Management, and their Use in Europe. Austrian Federal Environment Agency.

Bardos, R. P., Bone, B. D., Boyle, R., Evans, F., Harries, N. D., Howard, T., & Smith, J. W., 2016. The rationale for simple approaches for sustainability assessment and management in contaminated land practice. Science of the Total Environment, 563, 755–768.

Basu, N.B., Rao, P.S.C., Poyer, I.C., Annable, M.D., Hatfield, K., 2006. Flux-based assessment at a manufacturing site contaminated with trichloroethylene. J. Contam. Hydrol. 86, 105–127.

Bauer, P., Attinger, S., Kinzelbach, W., 2001. Transport of a decay chain in homogenous porous media; analytical solutions. J. Contam. Hydrol. 49, 217-239.

Bear, J., 1972. Dynamics of Fluids in Porous Media. Elsevier, New York.

Chambon, J.C., Binning, P.J., Jørgensen, P.R., Bjerg, P.L., 2011. A risk assessment tool for contaminated sites in low-permeability fractured media. J. Contam. Hydrol. 124, 82-98.

Chambon, J.C., Bjerg, P.L., Scheutz, C., Bælum, J., Jakobsen, R. and Binning, P.J., 2013. Review of reactive kinetic models describing reductive dechlorination of chlorinated ethenes in soil and groundwater. Biotechnol. Bioeng. 1, 1-23.

Chiang C.Y., Salanitro J.P., Chai E.Y., Colthart J.D., Klein C. L., 1989. Aerobic Biodegradation of Benzene, Toluene, and Xylene in a Sandy Aquifer – Data Analysis and Computer Modeling. Ground Water. 27, 823-834.

Christensen, A.G., Korsgaard A., Charlotte E.R., Johansen, P., 2002. Modeling of PCE transport and remediation in the unsaturated zone. Proceedings of the Third International Conference on Remediation of Chlorinated and Recalcitrant Compounds. Monterey, CA. May 2002. ISBN 1-57477-132-9.

Christophersen, M., Broholm, M., Mosbæk, H., Karapanagioti, H.K., Burganos, V.N., Kjeldsen, P., 2005. Transport of hydrocarbons from an emplaced fuel source experiment in the vadose zone at Airbase Værløse, Denmark. J. Contam. Hydrol, 81, 1- 33.

Ciriello, V., Lauriola, I., Bonvicini, S., Cozzani, V., Di Federico, V., Tartakovsky, D.M., 2017. Impact of hydrogeological uncertainty on estimation of environmental risks posed by hydrocarbon transportation networks, Water Resources Research, 53(11), 8686-8697.

Cremeans, M.M., Devlin, J.F., McKnight, U.S., Bjerg, P.L., 2018. Application of new point measurement device to quantify groundwater-surface water interactions, J. Contaminant Hydrology, 211, 85-93.

Danske regioner, 2017. I bund og grund. Regionernes arbejde med jordforurening: http://www.rn.dk/-/media/Rn_dk/Regional-Udvikling/Regional-Udvikling-sektion/Jordforurening/Inberetning-til-MST-og-Redeg%C3%B8relser-for-de-5-regioner/10213-Regionernes-arbejde-med-jordforurening---a%CC%8Arsrapport-2016_opslag.ashx?la=da

Davison, R., Hall, D.H., 2003. ConSim Version 2. User Manual. Golder Associates and UK Environment Agency. Golder Associates.

de Barros, F.P.J., Bolster, D., Sanchez-Vila, X., Nowak, W., 2011a. A divide and conquer approach to cope with uncertainty, human health risk, and decision making in contaminant hydrology, Water Resources Res., 47, W05508.

de Barros, F.P.J., Fiori, A., Bellin A., 2011b. A simple closed-form solution for assessing concentration uncertainty. Water Resources Research, Vol. 47, W12603.

European Environment Agency, 2015. Website: https://www.eea.europa.eu/data-and-maps/indicators/progress-in-management-of-contaminated-sites-3/assessment.

Falta, R.W., Stacy, M.B., Ahsanuzzaman, N.M., Wang, M., Earle, R.C., 2007. REMChlor. Remediation Evaluation Model for Chlorinated Solvents. User's Manual. Version 1.0. US EPA.

Fernandez-Garcia, D., Bolster, D., Sanchez-Vila, X., Tartakovsky, D.M., 2012. A Bayesian approach to integrate temporal data into probabilistic risk analysis of monitored NAPL remediation, Advances in Water Resources, 36, 108-120.

Fischer et al., 1979. Mixing in inland and coastal waters. ISBN-13: 978-0122581502.

Gelhar, L.W., Welty, C., Rehfeldt, K.R., 1992. A critical-review of data on field- scale dispersion in aquifers. Water Resour. Res. 28,1955–1974.

Grathwohl, P., Klenk, I.D., Maier, U., Reckhorn, S.B.F., 2002. Natural attenuation of volatile hydrocarbons in the unsaturated zone and shallow groundwater plumes: scenario-specific modelling and laboratory experiment. Groundwater Quality: Natural and Enhanced Restoration of Groundwater Pollution. Proceedings of the Groundwater Quality 2001 Conference held at Sheffield. UK, June 2001.

Harclerode, M.A., Macbeth, T.W., Miller, M.E., Gurr, C.J., Myers, T.S., 2016. Early decision framework for integrating sustainable risk management for complex remediation sites: Drivers, barriers, and performance metrics. J. Environmental Management, 184, 57-66.

Hunt, B., 1978, Dispersive Sources in Uniform, Ground Water Flow. J. Hydraulics Division. 104, 75-85.

Højberg et al., 2015. DK-model 2014 - Model opdatering og kalibrering. GEUS rapport 2015/8, København.

Hønning, J., Broholm, M.M., Bjerg, P.L., 2007. Role of diffusion in chemical oxidation of PCE in a dual permeability system. Environ. Sci. Technol. 41, 8426 – 8432.

Jørgensen, P.R., Hoffmann, M., Kistrup, J.P., Bryde, C., Bossi, R., Villholth, K.G., 2002. Preferential flow and pesticide transport in a clay-rich till: field, laboratory, and modeling analysis. Water Resour. Res. 38, 11.

Jørgensen, T.H., Schondelmaier, A.M., Jepsen, J.D., Holm, O.V., 2003. Forureningsundersø-gelse og afværgeprogram. Hovedrapport, Forurenet lokalitet nr. 461-169, Rugårdsvej 234 og 238 A-D, Odense, Fyns Amt, COWI.

Jørgensen, Torben H., Nielsen, L., Berger, H., Scheutz, C., Jakobsen, R., Bjerg, P.L., Durant, N., Cox, E., Mossing, C.H., Jacobsen, C.S., Rasmussen, P., 2007a. Forundersøgelser til pi-lotprojekt om stimuleret reduktiv deklorering. Miljøprojekt nr. 1146 2007..

Jørgensen, Torben H., Nissen, L., Nielsen, L., Hansen, M.H., Scheutz, C., Jakobsen, R., Bjerg, P.L., Durant, N., Cox, E., Mossing, C. H., Jacobsen, C. S., Rasmussen, P., 2007b. Pilotprojekt med stimuleret in situ reduktiv deklorering – Hovedrapport, Miljøprojekt Nr.1148, Kamath, R.K., Newell, C.J., Looney, B.B., Vangelas, K. M., Adamson, D. T., 2006. BIOBALANCE: A mass balance toolkit. For evaluating source depletion, competition effects, long-term sustainability, and plume dynamics. User's Manual. Groundwater Services Inc.

Københavns Amt, 2000. Virum Rens, Virumvej 84B, Virum. Supplerende undersøgelser. Københavns Amt, Teknisk Forvaltning Grundvandsafdelingen.. Udarbejdet af NIRAS. December, 2000.

Københavns Amt, 2001a. Virumvej 84B, Virum. Dataindsamling og modellering af stofspredning i umættet zone samt indledense modellering af forskellige afværgetiltag. Notat udarbejdet af NIRAS. 13, August, 2001.

Københavns Amt, 2001b. Virumvej 84B, Virum. Supplerende boring B12 – Afrapportering. Notat udarbejdet af NIRAS. December, 2001.

Lahvis, M.A., Baehr, A.L., Baker, R.J., 2004. Evaluation of volatilization as a natural attenuation pathway for MTBE. Ground Water. 42, 258–267.

Lima, G.D., Sleep, B.E., 2007. The spatial distribution of eubacteria and archaea in sand-clay columns degrading carbon tetrachloride and methanol. J. Contam. Hydrol. 94, 34 – 48.

Lu, C., Bjerg, P. L., Zhang, F., Broholm, M.M., 2011. Sorption of chlorinated solvents and deg-radation products on natural clayey tills. Chemosphere. 83, 1467–1474.

Lugg, G.A., 1968. Analytical Chemistry. 40(7): 1073, June 1968.

Luikov, A.V., Hartnett, J.P., 1968. Analytical Heat Diffusion Theory. Academic press, New York, N.Y

Mallants D., Espino A., Van Hoorick M., Feyen J., Vandenberghe N., Loy W., 2000. Dispersivity Estimates from a Tracer Experiment in a Sandy Aquifer. Ground Water, 38, 304-310.

McKay, L.D., Cherry, J.A., Gillham, R.W., 1993. Field experiment in a fractured clay till. 1. Hydraulic conductivity and fracture aperture. Water Resour. Res. 29, 1149-1162.

Miljøstyrelsen, 2016a. JAGG 2 - Vertikal transport ned til førstkommende betydende magasin. Miljøprojekt nr. 1828, 2016.

Miljøstyrelsen, 2017. GrundRisk. Coupling of vertical and horizontal transport models. Miljøprojekt nr. 1915, 2017.

Paladino, O., Moranda, A., Massabo, M., Robbins, G.A., 2018. Analytical solutions of three-dimensional contaminant transport models with exponential source decay, Groundwater, 56(1), 96-108.

Parker, B.L., Gillham, R.W., Cherry, J.A., 1994. Diffusive disappearance of immiscible-phase organic liquids in fractured geologic media. Ground Water. 32, 805–820.

RISC5, 2011. Risk-Integrated Software for Clean-ups. Version 5. User's Guide. April 2011.

Rivett M.O., Feenstra S., Cherry J.A.,1994. Transport of dissolved-phase plume from a residual solvent source in a sand aquifer, J Hydrol. 159, 27-41.

Robertson W.D., Cherry J.A., Sudicky E.A., 1991. Ground-Water Contamination from Two Small Septic Systems on Sand Aquifers, Ground Water. 29, 82-92.

Rotaru C., Ostendorf D.W., DeGroot D.J., 2014. Chloride Dispersion across Silt Deposits in a Glaciated Bedrock River Valley. J. Environ. Qual. 43, 459-467.

Saha, N., Rahman, M.S., Ahmed, M.B., Zhou, J.L., Ngo, H.H., Guo, W., 2013. Industrial metal pollution in water and probabilistic assessment of human health risk, J Environ Manage. 185, 70-78.

Scheutz, C., Durant, N.D., Dennis, P., Hansen, M.H., Jørgensen, T., Jakobsen, R., Cox, E.E., Bjerg, P.L., 2008. Concurrent Ethene Generation and Growth of Dehalococcoides Contain-ing Vinyl Chloride Reductive Dehalogenase Genes During an Enhanced Reductive Dechlo-rination Field Demonstration. Environ. Sci. Technol. 42, 9302-9309.

Scheutz, C., Broholm, M.M., Durant, N.D., Weeth, E.B., Jørgensen, T.H., Dennis, P., Jacobsen, C.S., Cox, E.E., Chambon, J.C., Bjerg, P.L., 2010. Field evaluation of biological enhanced reductive dechlorination of chloroethenes in clayey till. Environ. Sci. Technol. 44, 5134–5141.

Schulze-Makuch, 2005. Longitudinal Dispersivity Data and Implications for Scaling Behavior. Ground Water. 43, 443-456.

Schwede, R.L., Cirpka, O.A., 2010. Stochastic evaluation of mass discharge from pointlike concentration measurements, J. Contaminant Hydrology, 111(1-4), 36-47.

Simpson, M.J., Ellery, A.J., 2014. Exact series solutions of reactive transport models with generic initial conditions. Jounal of Hydrology 513, 7-12.

Sudicky E. A., Hwang H- T., Illman W. A., Wu Y. S., Kool J. B. & Huyakorn P., 2013. A semianalytical solution for simulating contaminant transport subject to chain-decay reactions. J. Contam. Hydrol. 144, 20-45.

Snow, D.T., 1969. Anisotropic permeability of fractured media. Water Resour. Res. 5, 1273–1289.

Spiegel, M.R., 1968. Mathematical handbook of formulas and tables. Schaum's outline series. McGraw-Hill.

Srinivasan, V., Clement, T.P., 2008a. Analytical solutions for sequentially coupled onedimensional reactive transport problems. Part I: Mathematical derivations. Adv. Water Resources. 31, 219–232.

Srinivasan, V., Clement, T.P., 2008b. Analytical solutions for sequentially coupled onedimensional reactive transport problems. Part II: Special cases, implementation and testing. Adv. Water Resources. 31, 203–218.

Sun, Y., Petersen, J.N., Clement T.P., 1999a. Analytical solutions for multiple species reactive transport in multiple dimensions, J. Contam. Hydrol. 35, 429-440.

Sun, Y., Petersen, J.N., Clement T.P., Skeen R.S., 1999b. Development of analytical solutions for multispecies transport with serial and parallel reactions, Water Resour. Res. 35, 185-190.

Thornton, S.F., 2017. Natural attenuation of hydrocarbons in groundwater. In : Consequences of Microbial Interactions with Hydrocarbons, Oils, and Lipids: Biodegradation and Bioremediation, Handbook of Hydrocarbon and Lipid Microbiology. Steffan, R. (ed.), Springer International Publishing, 3-1, p1-25.

Troldborg, M., Binning, P.J., Nielsen, S., Kjeldsen, P., Christensen, A.G., 2009. Unsaturated zone leaching models for assessing risk to groundwater of contaminated sites, J. Contam. Hydrol., 105(1-2), 28-37.

Troldborg, M., Nowak, W., Lange, I.V., Santos, M.C., Binning, P.J., Bjerg, P. L, 2012. Application of Bayesian geostatistics for evaluation of mass discharge .uncertainty at contaminated sites. Water Resour. Res. 48, w09535.

US EPA, 1996. Soil Screening Guidance: Technical Background Document, Second Edition. US EPA. EPA/540/R95/128.

van Genuchten, M.T, Alves, W.J., 1982. Analytical Solutions of the One Dimensional Convective-Dispersive Solute Transport Equation. United States Department of Agriculture. Agricultural research Service. Technical Bulletin, Number 1661.

Vanderborght, J., Vereecken, H., 2007. Review of dispersivities for transport modeling in soils. Vadose Zone Journal. 6, 29–52.

Verginelli, I., Baciocchi, R., 2013. Role of natural attenuation in modeling the leaching of contaminants in the risk analysis framework. J Environ Manage. 114, 395-403.

Wagner, J., Watts, S.A., Kent D.C., 1985. PLUME 3D: Three-Dimensional Plumes in Uniform Ground Water FlowRep. US EPA.

Wexler, E.L., 1992. Analytical Solutions for one-, two- and three-dimensional solute transport in ground-water systems with uniform flow. Chapter B7 in Techniques of Water-Resources Investigations of the United States Geological Survey. Book 3 Applications of Hydraulics. U.S. Department of the interior. U.S. Geological Survey. United States Government Printing Office, 1992.

Wiedemeier, T.H. Swanson, M.A, Moutoux, D.E., Gordon, E.K., Wilson, J.T., Wilson, B.H., Kampbell, D.H., Hansen, J.E., Haas, P., Chapelle, F.H., 1997. Technical Protocol for Evaluating Natural Attenuation of Chlorinated Solvents in Groundwater. Air Force Center for Environmental Excellence, Brooks Air Force Base, Texas, USA.

Wilson, R.D., Thornton, S.F. & Lerner, D.N., 2007. Forecasting natural attenuation as a risk-based groundwater remediation strategy Groundwater Science and Policy. Quevauviller, P. (ed), Royal Society of Chemistry, Ch. 7.2, p. 421-453.

Xu, M., Eckstein,Y., 1995. Use of weighted least-squares method in evaluation of the relationship between dispersivity and field scale. Ground Water. 33, 905-908.

Zarlenga, A., de Barros, F.P.J., Fiori, A., 2016. Uncertainty quantification of adverse human health effects from continuously released contaminant sources in groundwater systems, J Hydrology, 541, 850-861.